Article

Selective Growth of ZnO Nanorod Arrays on a GaN/Sapphire Substrate Using a Proton Beam Written Mask

H. L. Zhou, P. G. Shao, S. J. Chua, J. A. van Kan, A. A. Bettiol, T. Osipowicz, K. F. Ooi, G. K. L. Goh, and F. Watt

Cryst. Growth Des., **2008**, 8 (12), 4445-4448 • DOI: 10.1021/cg800267v • Publication Date (Web): 14 November 2008

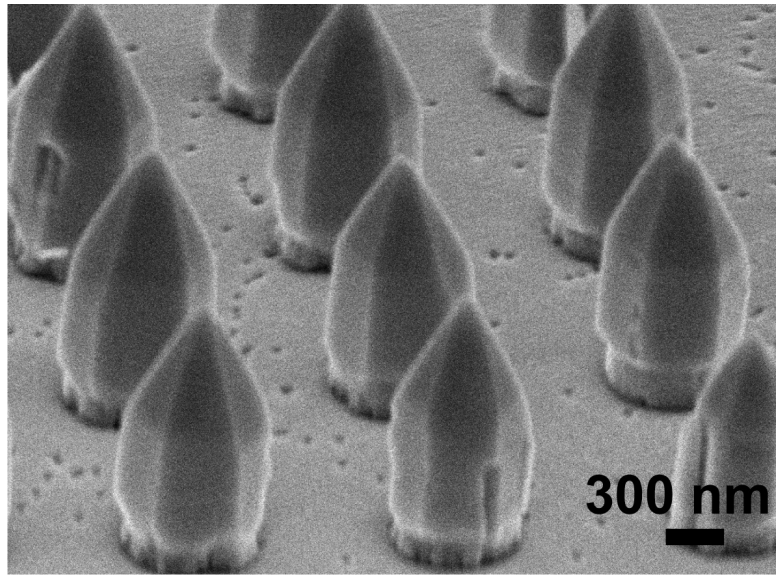

More About This Article

Additional resources and features associated with this article are available within the HTML version:

- Supporting Information
- Access to high resolution figures
- Links to articles and content related to this article
- Copyright permission to reproduce figures and/or text from this article

View the Full Text HTML

CRYSTAL GROWTH & DESIGN
2008
VOL. 8, NO. 12
4445–4448

Selective Growth of ZnO Nanorod Arrays on a GaN/Sapphire Substrate Using a Proton Beam Written Mask

H. L. Zhou,[†] P. G. Shao,[†] S. J. Chua,[‡] J. A. van Kan,[†] A. A. Bettiol,[†] T. Osipowicz,[†] K. F. Ooi,[‡] G. K. L. Goh,[‡] and F. Watt*,[†]

Centre for Ion Beam Applications, Department of Physics, National University of Singapore, 2 Science Drive 3, Singapore 117542, and Institute of Materials Research and Engineering, 3 Research Link, 117602 Singapore

Received March 13, 2008; Revised Manuscript Received August 28, 2008

ABSTRACT: ZnO nanorod arrays were grown on a GaN/sapphire substrate in a controllable way using a hydrothermal growth method. Proton beam writing (PBW), a direct-write 3D lithographic technique, was used to pattern a polymethyl methacrylate (PMMA) mask spin-coated on to a GaN substrate. ZnO, which has the same wurtzite crystal structure and a low lattice misfit of about 1.9% compared with GaN, nucleated and grew into vertical rods at positions where the GaN was exposed. The structural and optical characteristics of the ZnO nanorods were further investigated using X-ray diffraction (XRD), and microphotoluminescence spectroscopy (μ-PL). Annealing of the ZnO nanorods in nitrogen gas significantly improved the ultraviolet (UV) light emission at 380 nm wavelength, and successfully decreased the yellow and green band emission considerably. These results show new potential applications for devices based on ZnO nanostructures.

1. Introduction

ZnO has attracted considerable attention over the past years owing to its attractive properties, such as good piezoelectric characteristics, chemical stability, and biocompatibility, and its potential applications in optoelectronic switches, high-efficiency photonic devices, near-UV lasers, and complex three-dimensional nanoscale systems.[1−4] Recently, a number of methods have been used to produce one-dimensional (1D) ZnO nanostructures, such as thermal evaporation, catalyst-assisted vapor−liquid−solid (VLS), laser ablation, metal-organic chemical vapor deposition (MOCVD), and template-assisted and solution processes.[5−10]

For the case of ZnO nanoarray light emitters based on the quantum confinement effect, a big challenge is to control the dimension of ZnO nanostructures. Furthermore, the difficulty of p-type doping in ZnO has impeded the fabrication of ZnO homojunction devices. As an alternative approach to homojunction fabrication, a n-ZnO/*p*-GaN heterojunction has been suggested as a strong candidate for device applications.[11,12] Both ZnO and GaN have a fundamental bandgap energy in the range of about 3.3−3.4 eV, with the same wurtzite crystal structure, and a low lattice misfit of about 1.9%. Recently, Park reported on the fabrication of n-ZnO nanorod arrays vertically grown on p-GaN and demonstrated the potential to realize photonic and electronic nanodevices.[13] In addition, random lasing was reported in ZnO nanoparticles,[14,15] nanoneedles,[16] nanorods,[17] and nanowires.[18] If we can realize vertically aligned ZnO nanostructures with controllable size and position, it will be helpful for achieving stimulated emission from such structures. Meanwhile, another challenge to researchers is achieving large-area well-aligned nanostructures by other cost-effective growth methods rather than by the MOCVD and VLS techniques. One of the most cost-effective methods, the hydrothermal method,[19,20] has a process temperature as low as 80−100 °C, and because of this low process temperature, polymers such as PMMA can be used as a mask.

To fabricate nanostructures in a controllable way, it is critical to fabricate a high quality mask with dimensions at the nano scale. In the past decade, nano fabrication technology has developed at an astonishing speed, mainly driven by IC industry. Technologies such as electron beam writing, proton beam writing (PBW) and focused ion beam (FIB) lithography have shown their potential in nano fabrication and have been considered as promising technologies for next generation lithographies.[21−23] Among these technologies, PBW has exhibited the ability to fabricate 3D structures down to the 20 nm level in resist materials such PMMA, SU8 and hydrogen silsesquioxane $(HSiO_{3/2})_8$ HSQ. The advantages of PBW is that high aspect ratio masks can be directly fabricated, exhibiting vertical structures, low edge roughness and relative large mask thickness.[22,23] These characteristics are due to the high mass of the proton compared with the electron, resulting in deeper and straighter penetration into the resist. The efficiency of PBW is higher than FIB, which essentially is a sputtering process, and is therefore more suitable for large area fabrication. However, as a direct writing process, PBW is a serial process and as such is not suitable for mass production compared with masked lithography as in the integrate circuit (IC) industry. However, PBW is efficient for scientific research and prototype development, where only a few prototype devices are required.

2. Experimental Methods

In this work, we have investigated the fabrication of ZnO nanorod arrays using the hydrothermal process on GaN/sapphire (0001) substrates covered with a PBW structured PMMA mask. The GaN/sapphire substrate was prepared by depositing about 2.0 μm thick GaN films on *c*-plane sapphire substrates with low-temperature GaN buffer layers by MOCVD. Trimethyl-Gallium and ammonia (NH_3) were used as the sources of Ga and N, respectively, with H_2 as carrier gas. Then a 300 nm thick PMMA layer was spin coated on the GaN/sapphire substrates, circular hole array patterns were fabricated in the PMMA layer using a 2 MeV proton beam and the patterned structures are shown in Figure 1. The whole pattern size is 25 μm × 25 μm with holes of 400 nm in diameter. 200 × 200 μm^2 squares were also patterned on the PMMA layer on the same substrate as a control to observe the

* Corresponding author. Present address: Department of Electronics and Telecommunications, Norwegian University of Science and Technology, NO-7491 Trondheim, Norway. E-mail: hailong.zhou@iet.ntnu.no.
[†] National University of Singapore.
[‡] Institute of Materials Research and Engineering.

10.1021/cg800267v CCC: $40.75
Published on Web 11/14/2008

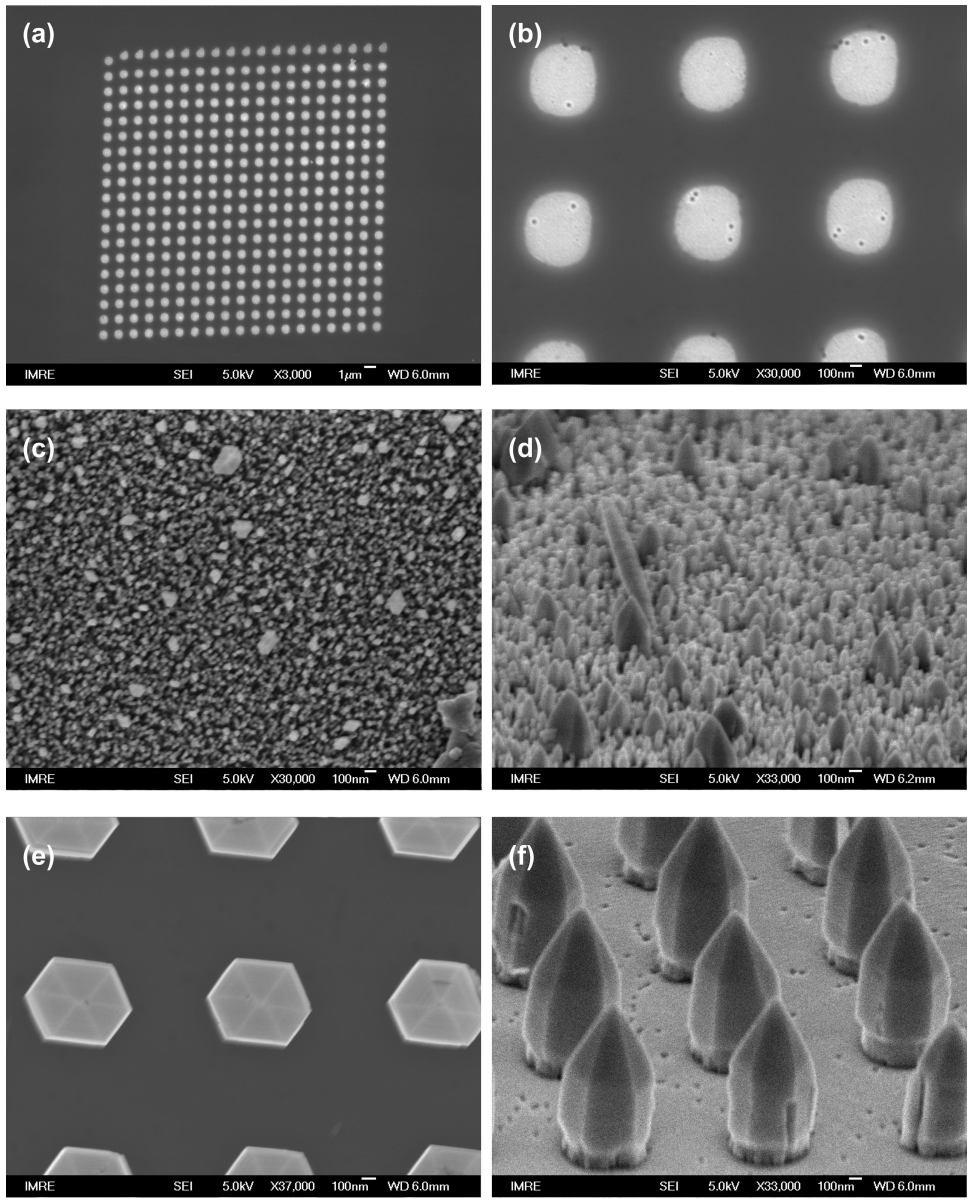

Figure 1. (a) Low- and (b) high-magnification SEM images showing the proton beam written PMMA template; (c, d) SEM images of ZnO nanorod arrays grown on GaN/sapphire without the patterned mask; (e) SEM top-view image of the ZnO nanorod arrays selectively grown using the patterned PMMA template; (f) SEM birds-eye view image of the ZnO nanorod array showing its 3D characteristics.

large area ZnO growth under the same conditions. The patterned templates were then placed in a 90 °C nutrient solution for the growth of ZnO nanorods.[14] The nutrient solution was prepared from an aqueous solution containing $Zn(NO_3)\cdot 6H_2O$ (Aldrich, Milwaukee, WI) and $NH_4NO_3\cdot 2H_2O$ (Aldrich, Milwaukee, WI) in deionized water at a concentrations of 0.026 and 0.3 mol L^{-1}, respectively. Sufficient ammonium hydroxide was then added immediately to increase the pH of the solution and initiate the growth of ZnO. The amount of ammonium hydroxide added was calibrated by raising the pH of a room-temperature solution to 9.5.

The position of the ZnO nanostructures is determined by the PMMA mask, and the diameter and length of ZnO nanostructures are controlled by using specific mask pattern sizes. After 10 h growth the substrate was removed from the nutrient solution and placed in acetone to dissolve the resist mask layer. Finally the sample was annealed in nitrogen gas at 500 °C for 20 min.

Structural and optical characteristics of as-grown ZnO nanorod arrays were investigated using X-ray diffraction (XRD), field emission scanning electron microscopy (FE-SEM), and microphotoluminescence (μ-PL). The morphology of the ZnO/GaN/ sapphire samples was studied using a SEM (JEOL JSM-6700F, 5kV), and the XRD spectrum of the ZnO nanorod array sample was taken with a Bruker D8 GADDS X-ray diffractometer using the Cu $K\alpha_1$ line. The μ-PL spectra were recorded at room temperature using the 325 nm excitation line (Renishaw 2000) from a He−Cd laser, using a focused laser beam with a lateral resolution of 2.0 μm.

3. Results and Discussion

As shown in images c and d in Figure 1, large-area ZnO growth resulted in crowded columns, most of which are aligned vertically to the substrate with different diameters ranging from several tens to a few hundred nanometers and with different heights. Those with larger diameter in general exhibited larger heights and showed an obvious sharp tip at the top. In contrast, when using the nano array mask, the ZnO grew into uniform hexagonal structures exhibiting a pyramidal tip with a similar cross-sectional size as defined by the diameter of the holes in the mask. As shown in images e and f in Figure 1, the average diameter of the ZnO nanorods was about 400 nm. The rods were also observed to be of uniform height, about 1.5 μm.

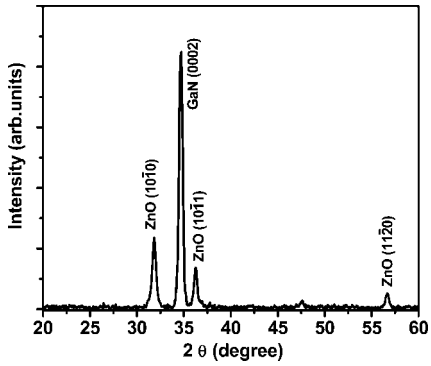

Figure 2. X-ray diffraction patterns of ZnO nanorod arrays.

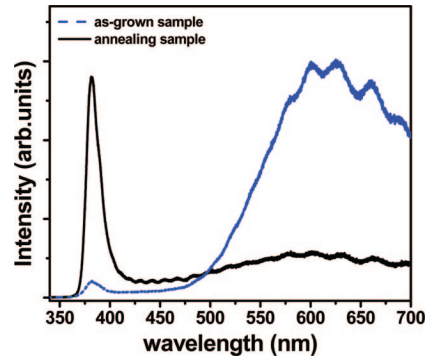

Figure 3. Room-temperature photoluminescence spectra of the as-grown ZnO nanorods (dash line) and nanorods annealed in nitrogen ambient (black line).

Because there is no agitation in the solution, the unpatterned large area growth is limited by ion diffusion. In the nano array area, the holes cover around 15% of the surface area, and so in this area there are relatively more ions available for growth. This results in ZnO nano pillars of increased height.

From Figure 1d, it can be seen from unpatterned growth the aspect ratios of the ZnO nano rods vary within a range of 3−5, with the smaller crystals exhibiting higher ratios. In the nano array area, the aspect ratio is 3, see Figure 1f. It can also be seen in Figure 1d that the effective crystal nucleus density on the GaN substrate is about 100/μm^2. Therefore, when the crystals grow to a size of about 60nm in diameter which corresponds to a height of 180−300 nm, the crystals which are in the same crystal orientation, meet and combine to form large single crystals. Each crystal inside the nano mask hole was initially formed from many small crystals which joined and grew into a 1.5 μm high rod. This hypothesis is supported by the Figure 1f, which shows that the base of each of the large crystal rods consists of many smaller crystal rods.

It should be noted that some crystals might nucleate at defects on the substrate and therefore are not vertical to the substrate, as can be seen in Figure 1d, which shows that some pillars are not orientated perpendicular to the surface.

As shown in images e and f in Figure 1, the cross-section of these ZnO rods are hexagonal, and the rods are perpendicular to the substrate with the same orientation alignment, indicating that the rods grow along the [0001] direction, with the (0001) crystal planes matching the (0001) planes of the substrate GaN. The rods are uniform in size with diameters around 400 nm, and are separated by an equal inter-rod distance of 700 nm, which matches the size of the original PBW pattern as show in images a and b in Figure 1.

The crystalline phase of the ZnO nanorods was analyzed by XRD. Figure 2 shows that the nanorods have good crystallinity, exhibiting a hexagonal structure. The three labeled diffraction peaks at $2\theta \approx 31.6°$, ~36.3, and ~56.6° correspond to the (10$\bar{1}$0), (10$\bar{1}$1), and (11$\bar{2}$0) facets in the wurzite ZnO structure. The presence of a range of ZnO XRD peaks apart from the (0002) peak in the data (Figure 2) for the *c*-axis oriented nanorods array sample may be explained by the fact that the size of the X-ray beam is about 3 × 3 mm^2 and thus, because the entire size of the PMMA patterned area is 25 × 25 μm^2, i.e., much smaller than the XRD beam size, the XRD is sampling areas beyond the PMMA template, where the growth on the opening area of GaN template might have occurred and will be as in images c and d in Figure 1, i.e., much less well aligned, leading to the presence of these other XRD reflection peaks. The ZnO (0002) peak is not observed because of the overlapping strong (0002) peak of the GaN substrate. The sharp diffraction peaks of ZnO indicate that the as-grown nanorods are highly crystalline.

The micro-PL spectra measured at room temperature from the as-grown ZnO nanorod arrays before and after annealing are shown in Figure 3. Strong improvement in the PL for the hydrothermal grown ZnO nanorods was observed after postannealing treatment with nitrogen gas. The UV exciton emission was observed at 381.7 nm with a full width at half-maximum (fwhm) of 14 nm of as-grown ZnO nanorods compared with the fwhm of 11.6 nm of the annealed sample. The fwhm value for the ZnO nanorods after annealing is superior to that of ZnO nanorods on a GaN substrate grown by the VLS process.[25] In addition, the intensity of the UV emission was found to be increased by around 1 order of magnitude after annealing.

It is well-known that the excited light emission intensity is determined by both the radiative and nonradiative recombinations. Because the as-grown ZnO nanorods were prepared by the hydrothermal method, the growth temperature is much lower than other growth methods (e.g., MOCVD, MBE, thermal evaporation, etc.). Because it is generally acknowledged that such lower-temperature techniques could introduce excess zinc or oxygen vacancies, these defects could act as nonradiative centers and reduce light emission. In our case, both crystal defects and surface defects could be minimized. As observed in Figure 3, a weak UV light emission peak and strong visible light emission was observed from the as-grown ZnO before annealing. To reduce and restructure nonradiative related defects, we chose an annealing temperature of 500 °C,[27,28] resulting in increased luminescence efficiency. Our results indicate that the ZnO nanorods fabricated in this study were of high optical quality. On the other hand, the as-grown nanorods exhibited yellow-green emission centered at ~600 nm, commonly observed in hydrothermally grown ZnO nanorods.[24,26] This yellow-green band was observed to be highly suppressed after the annealing treatment. In ZnO nanorods annealed under N-rich conditions, oxygen desorption may occur and oxygen vacancies could be formed. A decreased intensity at 600 nm is observed after annealing in nitrogen, indicating that the yellow-green emission is not directly attributed to oxygen vacancy defects, a result which agrees with the conclusion of Kwok et al. and Sim et al. [27,28]

4. Conclusion

In summary, we have demonstrated the controlled growth of ZnO nanorod arrays using the hydrothermal growth method. The PMMA template on which the nanorods were grown was

made by proton beam writing, which is a new 3D direct write technique of high precision. The highly ordered vertical aligned nanorods have uniform hexagonal structure with a diameter of around 400 nm, dictated by the template pattern feature size. The observed height of the nanorods was about 1.5 μm. After annealing, the nanorod arrays made using this technique are highly crystalline and are of excellent optical quality. We have shown that this fabrication process offers a simple and efficient method to fabricate ordered nano arrays of controlled dimensions, and has high potential in the development of vertical nanorod devices.

Acknowledgment. H.Z. acknowledges support from the NUS Academic Research Fund. We also acknowledge the help coming from CIBA Laboratory of Physics Department NUS and Mr. Lim Poh Chong of the Institute of Materials Research & Engineering.

References

(1) Xia, Y. N.; Yang, P. D.; Sun, Y. Y.; Wu, B.; Yin, Mayers, Y.; Kim, F.; Yan, H. *Adv. Mater.* **2003**, *15*, 353.
(2) Pan, Z. W.; Dai, Z. R.; Wang, Z. L. *Science* **2001**, *291*, 1947.
(3) Hu, J.; Odom, T. W.; Lieber, C. M. *Acc. Chem. Res.* **1999**, *32*, 435.
(4) Chen, C. S.; Kuo, C. T.; Wu, T. B.; Lin, I. N. *Jpn. J. Appl. Phys.* **1997**, *36*, 1169.
(5) Huang, M.; Mao, S.; Feick, H.; Yan, H.; Wu, Y.; Kind, H.; Weber, E.; Russo, R.; Yang, P. D. *Science* **2001**, *292*, 1897.
(6) Kong, Y. C.; Yu, D. P.; Zhang, B.; Fang, W.; Feng, S. Q. *Appl. Phys. Lett.* **2001**, *78*, 407.
(7) Wu, J. J.; Liu, S. C. *Adv. Mater.* **2002**, *14*, 215.
(8) Zheng, M. J.; Zhang, L. D.; Li, G. H.; Shen, W. Z. *Chem. Phys. Lett.* **2002**, *363*, 123.
(9) Shen, G. Z.; Bando, Y.; Lee, C. J. *J. Phys. Chem. B* **2005**, *109*, 10578.
(10) Li, Y. B.; Bando, Y.; Golberg, D. *Appl. Phys. Lett.* **2004**, *84*, 3603.
(11) Vispute, R. D.; Talyansky, V.; Choopun, S.; Sharma, R. P.; Vekatesan, T.; He, M.; Tang, X.; Halpern, J. B.; Spencer, M. G.; Li, Y. X.; Salamanca-Riba, L. G.; Iliadis, A. A.; Jones, K. A. *Appl. Phys. Lett.* **1998**, *73*, 348.
(12) Hong, S. K.; Hanada, T.; Makino, H.; Chen, Y.; Ko, H.-J.; Yao, T.; Tanaka, A.; Sasaki, H.; Sato, S. *Appl. Phys. Lett.* **2001**, *78*, 3349.
(13) Park, W. I.; Yi, G. C. *Adv. Mater.* **2004**, *16*, 87.
(14) Stassinopoulos, A.; Das, R. N.; Giannelis, E. P.; Anastasiadis, S. H.; Anglos, D. *Appl. Surf. Sci.* **2005**, *247*, 18.
(15) Lau, S. P.; Yang, H. Y.; Yu, S. F.; Yuen, C.; Leong, E. S. P.; Li, H. D.; Hng, H. H. *Small* **2005**, *1*, 956.
(16) Lau, S. P.; Yang, H. Y.; Yu, S. F.; Li, H. D.; Tanemura, M.; Okita, T.; Hatano, H.; Hng, H. H. *Appl. Phys. Let.* **2005**, *87*, 013104.
(17) Yu, S. F.; Yuen, C.; Lau, S. P.; Park, W. I.; Yi, G.-C. *Appl. Phys. Lett.* **2004**, *84*, 3241.
(18) Hsu, H. C.; Wu, C. Y.; Hsieh, W. F. *J. Appl. Phys.* **2005**, *97*, 064315.
(19) Andeen, D.; Kim, J. H.; Lange, F. F.; Goh, Gregory, K. L.; Tripathy, S. *Adv. Funct. Mater.* **2006**, *16*, 799.
(20) Yamabi, S.; Imai, H. *J. Mater. Chem.* **2002**, *12*, 3773.
(21) Madou, Marc J. *Fundamentals of Microfabrication: The Science of Miniaturization*, 2nd ed.; CRC Press: Boca Raton, FL, 2002; p 320.
(22) van Kan, J. A.; Bettiol, A. A.; Watt, F. *Nano Lett.* **2006**, *6*, 579.
(23) Watt, F.; van Kan, J. A.; Rajta, I.; Bettiol, A. A.; Choo, T. F.; Breese, M. B. H.; Osipowicz, T. *Nucl. Instrum. Methods, B* **2003**, *210*, 14.
(24) Greene, L. E.; Law, M.; Goldberger, J.; Kim, F.; Johnson, J. C.; Zhang, Y.; Saykally, R. J.; Yang, P. D. *Angew. Chem., Int. Ed.* **2003**, *42*, 3031.
(25) Wang, X. D.; Song, J. H.; Li, P.; Ryou, J. H.; Dupuis, R. D.; Summers, C. J.; Wang, Z. L. *J. Am. Chem. Soc.* **2005**, *127*, 7920.
(26) Li, D.; Leung, Y. H.; Djurišić, A. B.; Liu, Z. T.; Xie, M. H.; Shi, S. L.; Xu, S. J.; Chan, W. K. *Appl. Phys. Lett.* **2004**, *85*, 1601.
(27) Kwok, W. M.; Djurišić, A. B.; Leung, Y. H.; Li, D.; Tam, K. H.; Phillips, D. L.; Chan, W. K. *Appl. Phys. Lett.* **2006**, *89*, 183112.
(28) Sim, A.Y. L.; Goh, G. K. L.; Tripathy, S.; Andeen, D.; Lange, F. F. *Electrochim. Acta* **2007**, *52*, 2933.

CG800267V